Open-State Models of a Potassium Channel

Philip C. Biggin and Mark S. P. Sansom
Laboratory of Molecular Biophysics, Department of Biochemistry, The University of Oxford, Oxford OX1 3QU, United Kingdom

ABSTRACT The structure of the bacterial potassium channel, KcsA, corresponds to the channel in a closed state. Two lines of evidence suggest that the channel must widen its intracellular mouth when in an open state: 1) internal block by a series of tetraalkylammonium ions and 2) spin labeling experiments. Thus it is known that the protein moves in this region, but it is unclear by how much and the mechanisms that are involved. To address this issue we have applied a novel approach to generate plausible open-state models of KcsA. The approach can be thought of as placing a balloon inside the channel and gradually inflating it. Only the protein sees the balloon, and so water is free to move in and out of the channel. The balloon is a van der Waals sphere whose parameters change by a small amount at each time step, an approach similar to methods used in free energy perturbation calculations. We show that positioning of this balloon at various positions along the pore axis generates similar open-state models, thus indicating that there may be a preferred pathway to an open state. We also show that the resulting structures from this process are conformationally unstable and need to undergo a relaxation process for up to 4 ns. We show that the channel can relax into a new state that has a larger pore radius at the region of the intracellular mouth. The resulting models may be useful in exploring models of the channel in the context of ion permeation and blocking agents.

INTRODUCTION

Ion channels are found in a wide variety of cells and have diverse biological roles (Hille, 1992). The causes of an increasing number of diseases are being identified as malfunctioning ion channels (Ashcroft, 2000). The recent x-ray structure of a bacterial potassium channel, KcsA (Doyle et al., 1998), offers insights into how the functional properties of such channels are related to their three-dimensional structures. The basic structure of KcsA is a tetramer of a simple transmembrane fold made up an M1 helix spanning the bilayer, a P-region looping back into the membrane made up of a short P-helix, and an extended selectivity filter, followed by a second membrane-spanning M2 helix. In this context it is of some importance that KcsA shares structural homologies with voltage-gated potassium (Kv) channels of higher organisms (MacKinnon et al., 1998), although there may be significant details in their gating mechanisms (Camino et al., 2000).

Both experimental and computational data suggest that the x-ray structure of KcsA may correspond to a closed state of the channel. Three different sets of experiments support this view. Blocking experiments with tetraalkylammonium ions on Kv channels (Armstrong and Binstock, 1965; Armstrong, 1971, 1997) and more recently on KcsA (Heginbotham, 2001; Zhou et al., 2001) suggest that these large organic cations can enter the central cavity of the K channel via the intracellular mouth when the channel is open. However, simple comparison of the KcsA structure with the radii of such blockers indicates that they could not pass through the intracellular mouth when the channel is in its x-ray conformation. The second set of experiments use site-directed spin labeling and electron paramagnetic resonance (EPR) spectroscopy to probe changes in the structure of KcsA upon lowering the pH (Perozo et al., 1998, 1999), a change in conditions known to promote the open state of the channel (Meuser et al., 1999; Heginbotham et al., 1999). These suggested movement of the M2 helices of KcsA so as to open up the intracellular mouth of the channel. A third set of experiments using cyclic nucleotide-gating channels also lends support to the idea of movement in this region. Using a histidine scan of the post S6 region of a cyclic nucleotide-gating channel, Zagotta and colleagues (Flynn and Zagotta, 2001; Johnson and Zagotta, 2001) have shown that this channel also undergoes changes in conformation in this part of the protein during opening. Finally, a number of theoretical studies (Allen et al., 2000; Roux et al., 2000; Biggin et al., 2001) have indicated that the narrow hydrophobic intracellular mouth of KcsA forms an energetic barrier to ion permeation and that widening of this mouth could help to remove that barrier.

Although these various studies indicate that the KcsA channel undergoes a conformational change, they do not provide a precise indication of the nature of the movement of, e.g., the M2 helices. What is needed is a modeling procedure that can generate a stable open conformation of the channel that is guided by experimental data but that is relatively unbiased as to the nature of the final open state. Ideally one would like to be able to run, e.g., a molecular dynamics (MD) simulation for long enough to observe the gating events in real time. However, despite recent improvements in simulations of membrane systems (Forrest and Sansom, 2000) the time scale of gating events, which is on the order of microseconds, is still beyond current computa-

Submitted February 13, 2002, and accepted for publication June 19, 2002.

Address reprint requests to Dr. Philip C. Biggin, Laboratory of Molecular Biophysics, Department of Biochemistry, The University of Oxford, The Rex Richards Building, South Parks Road, Oxford OX1 3QU, UK. Tel.: 44-1865-275380; Fax: 44-1865-275182; E-mail: phil@biop.ox.ac.uk.

0006-3495/02/10/1867/10 $2.00

TABLE 1 Summary of simulations

Simulation	Starting structure	Z (Å)	σ (Å)	Duration (ns)
Ex1	Closed	−14	5	1
Ex2	Closed	−14	7	1
Ex3	Closed	−14	9	1
Ex4	Closed	−9.5	9	1
Ex5	Closed	−11.0	9	1
Ex6	Closed	−12.5	9	1
Ex7	Closed	−15.5	9	1
Rx1	End structure from Ex3			11
Rx2	End structure from Ex4			5
Rx3	End structure from Ex7			5

The closed structure is that at the end of 1-ns simulation in POPC, starting from the x-ray structure of KcsA.

tional resources. Therefore, in this paper we use a steered MD approach (Isralewitz et al., 2001; Grubmuller et al., 1996) to explore possible open state(s) of KcsA.

METHODS

MD simulations

All simulations were performed with GROMACS (Berendsen et al., 1995) using the Gromos87 force field and were for 1 ns unless otherwise stated. The time step was 2 fs, and coordinate frames were saved to disk every 1 ps. Long-range electrostatic interactions were calculated using PME (Procacci et al., 1996). The system was coupled to an external heat bath (Berendsen et al., 1984), at 300 K with $\tau_T = 0.1$ ps, and the system was pressure-coupled with $\tau p = 1.0$ ps and a reference pressure of 1 bar. The LINCS (Hess et al., 1997) algorithm was used in the maintenance of bond lengths and the simple point charge water model (Hermans et al., 1984) was used. All calculations were performed on a Linux PC cluster constructed in house with eight dual Pentium III 633-Mhz CPUS. Redhat 6.2 with kernel 2.2.14–12smp was used.

Generation of open-channel models

The starting point for our simulations was a closed state of the channel, corresponding to the structure at $t = 1$ ns of a simulation of KcsA in a POPC lipid bilayer, based upon previous work from this laboratory (Shrivastava and Sansom, 2000). Thus, the simulation system consisted of a KcsA tetramer, 243 1-palmitoyl-2-oleoyl-*sn*-glycero-3-phosphocoline lipid molecules, 9835 simple point charge water molecules, and 3 Cl^- counterions. Potassium ions in the filter region and one in the cavity were present throughout all of the simulations. The steered MD process used to generate candidate open-state structures used the λ parameter (more often associated with free energy perturbation calculations) to progressively expand a van der Waals sphere somewhere within the gate region of the channel. This is reminiscent of inflating a balloon positioned within the pore. The van der Waals sphere was defined in the standard fashion by two parameters, σ and ϵ. As the value of λ was increased from 0 to 1 during the course of a simulation, σ was increased from 1.33 Å (equivalent to a K^+ ion in radius) to the final value given in Table 1, whereas ϵ remained constant at 0.00714 kcal/mol. During the simulations the van der Waals sphere did not interact with water molecules, only with protein atoms. Thus additional water molecules were free to move into the expanding channel.

In the various simulations (Table 1), the expanding van der Waals sphere was centered at various positions along the pore (z) axis from $z = -9.5$ Å (corresponding to the intracellular end of the central cavity) to $z = -15.5$ Å (corresponding to the limit of α-helicity on the M2 segment of the protein) as indicated in Fig. 1. We did not place a sphere any higher up the channel (i.e., further toward the selectivity filter) as we wanted to restrict the perturbation to the lower part of the channel. A sphere too near the filter would obviously cause quite drastic disruption of the integrity of the filter region, and we were primarily interested in seeing whether the lower gate region could move independently of the filter. In addition, in simulations Ex1 to Ex3, the final size (i.e., final σ value) of the sphere was varied.

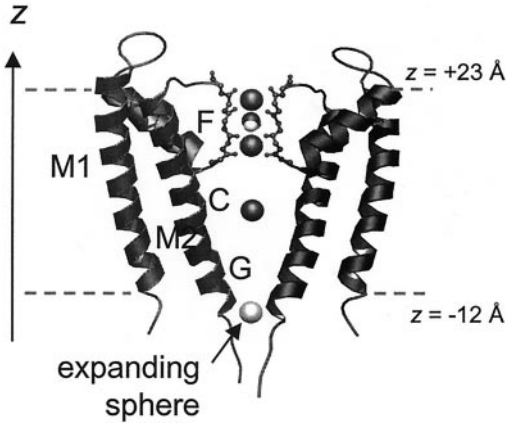

FIGURE 1 Schematic diagram of the simulation system. For clarity, only two of the four KcsA subunits are shown, with the backbone atoms of the TVGYG selectivity filter highlighted in ball-and-stick format. The three large dark spheres represent potassium ions, with a water molecule separating the two potassium ions in the filter. The light gray sphere indicates one of the starting positions for the expanding "balloon". The broken horizontal lines indicate the approximate location of the bilayer/water interfaces.

This initial stage gave us a set of expanded open-state models. To explore the stability of such models it was necessary to relax the protein. To explore this, starting from the channel structures generated at the end of simulations Ex3, Ex4, and Ex7 we performed a further 5-ns (and in the case of Ex3, 11-ns) simulation during which the sphere was removed from the protein. Thus in the following analysis we had three classes of models: 1) closed, i.e., similar to the x-ray conformation; 2) expanded, i.e., as yielded by the 1-ns simulations (Ex3 to Ex7) with the expanding sphere; and 3) relaxed, i.e., at the end of the 5-ns (and 11-ns) Rx1–3 simulations in the absence of the expanding sphere.

Analysis

Pore radius profiles were analyzed using HOLE (Smart et al., 1993, 1996). Born energies were calculated using UHBD (Davis et al., 1991) as the solvation energy of the ion within the protein compared with that within bulk solvent. Secondary structure analysis used DSSP (Kabsch and Sander, 1983). Analysis of hinge bending used Hingefind (Wriggers and Schulten, 1997) and Dyndom (Hayward et al., 1997; Hayward and Berendsen, 1998). Molecular structure diagrams were generated using VMD (Humphrey et al., 1996), Molscript (Kraulis, 1991), and POV-Ray. Tetra-alkylammonium ions were simulated in a box of water for 1 ns each and the radius of gyration extracted as a mean over the length of the simulation.

RESULTS

Characterization of the expanded channel models

All five of the models generated by the expansion phase using $\sigma = 9$ Å (i.e., Ex3 to Ex7) showed a similar defor-

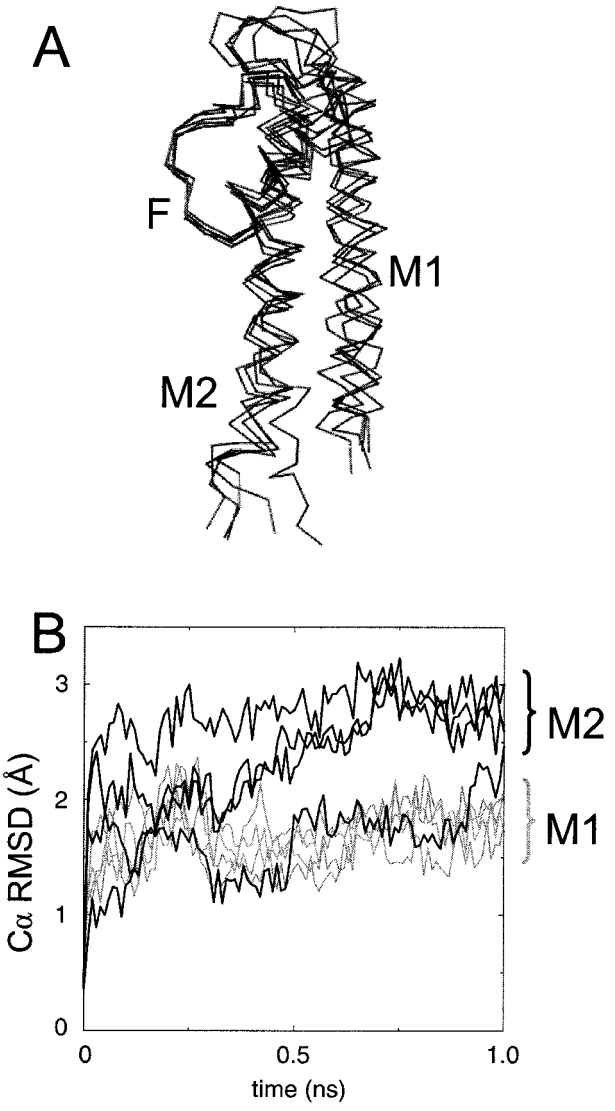

FIGURE 2 (*A*) Comparison of the five final structures of simulations Ex3 to Ex7 (see Table 1) after the expansion phase (see Table 1). One chain of each of the five final expanded structures is least-squares fitted on the superimposed Cα atoms of the TVGYG selectivity filter (F). (*B*) Cα RMSDs versus time for the M1 (*gray lines*) and M2 (*black lines*) helices during simulation Ex7.

mation and appeared to accommodate the expanding sphere in a similar fashion. Furthermore, during all of the expansion simulations, water was observed to enter into the channel. Ex1 and Ex2 appeared to yield incompletely expanded structures and so were excluded from further analysis. In Fig. 2 *A* we show an overlay of the final frames (one chain only) by a least-squares fit onto the Cα carbons of the TVGYG motif in the filter region. Most of the changes relative to the closed (i.e., $t = 0$) structure appear to be localized to the intracellular half of the protein, with the filter region remaining in the same conformation. A more detailed analysis of the root mean square deviations (RMSDs; Fig. 2 *B*) revealed that in the expansion simulations, 1) the M2 helices move more than that M1 helices and 2) the M2 helices do not move away from each other in a symmetrical fashion. Rather, we observe one or more of the helices moving with respect to the position of the others. Similar behavior has been seen in occasional spontaneous openings of the channel seen in long MD simulations (Shrivastava and Sansom, 2002).

To better characterize this movement we used Hingefind (Wriggers and Schulten, 1997) in conjunction with VMD (Humphrey et al., 1996) to give an indication of how the protein accommodated the expanding sphere. This may reveal those regions of the channel that preferentially undergo conformational changes under the strain of the expanding sphere. The Hingefind results (summarized in Table 2) indicate that the channel opens via a hinge axis located consistently around the Gly104 region of the protein. This axis runs parallel to the Gly104/Leu105 Cα-Cα bond. As might be anticipated, there is a degree of error in estimation of the hinge location for a relatively small (Cα RSMD $\sim$2.8 Å) degree of conformational change and perhaps should only be taken as a suggestion that the channel could bend in that region when it opens. However, it is interesting that the region from G99 to G104 has also been seen to be distorted from ideal α-helicity both in simulations of isolated M2 helices (Shrivastava et al., 2000) and in long MD simulations of KcsA that exhibit occasional spontaneous openings (Shrivastava and Sansom, 2002). A typical result of this analysis is illustrated in Fig. 3, which indicates the location of the effective hinge axis and how the protein moves in relation to it. It is interesting to note that the movement is best characterized by a hinge that allows the M2 helix to move in a direction that combines both a tangential and a radial element relative to the pore. We also analyzed potential domain movements with the program Dyndom (Hayward et al., 1997; Hayward and Berendsen, 1998). This gave comparable results, in terms of the location and direction of the hinge axis. This gives us some confidence that the description of the conformational change is not too sensitive to the method of analysis used to describe it.

Analysis of the α-helical content of the protein during the expansion simulations revealed that the mean α-helical content of the protein during the simulations was 69.6% $\pm$ 0.5%, compared with 65% for the crystal structure. During all of the simulations there was little if any loss of secondary structure as the pore was expanded. This suggests that the helix can gently distort to accommodate the expanding sphere by concerted small changes in backbone torsion angles rather than form a highly localized kink with loss of hydrogen bonding at a hinge residue in the M2 helix. This is supported by detailed comparison of the backbone torsion angles for the various expanded models. Indeed, if anything, the backbone torsion angles in the latter are closer to canonical α-helical values than in the original x-ray structure.

TABLE 2 Hingefind analysis

	Closest Cα to pivot point*	Comment on axis†	Rotation angle (°)	Deviation‡ (°)
Ex4 ($z = -9.5$ Å)				
Subunit A	T101 (5.3)	I100-T101	13	34
Subunit B	A108 (2.3)	I100-T101	18	7.5
Subunit C	No movement			
Subunit D	No movement			
Ex5 ($z = -11.0$ Å)				
Subunit A	A32 (4.6)	G104-L105	16	11.5
Subunit B	L81 (3.8)	T85-L86	20	31.6
Subunit C	A32 (2.0)	A108-A109	16	23.4
Subunit D	H25 (6.1)	G104-L105	9	56.1
Ex6 ($z = -12.5$ Å)				
Subunit A	A29 (2.6)	No assignment	28	0.7
Subunit B	L105 (3.4)	G014-L105	23	14.21
Subunit C	A28 (4.5)	No assignment	10	10.7
Subunit D	V97 (5.5)	No assignment	5	60.3
Ex3 ($z = -14.0$ Å)				
Subunit A	A28 (0.0)	G104-L105	22	16.2
Subunit B	L105 (5.0)	G105-L105	20	0.5
Subunit C	W113 (3.3)	No assignment	23	4.9
Subunit D	No movement			
Ex7 ($z = -15.5$ Å)				
Subunit A	No movement			
Subunit B	>10 away	No assignment	7	33.4
Subunit C	A29 (2.4)	R27-A28	12	28.8
Subunit D	A28 (4.1)	A31-A32	17	10.3

*A pivot point is defined by Hingefind in three-dimensional space. The residues in this column indicate the nearest Cα atom and its distance (in angstroms) from that point.

†To give an indication of where in space the hinge axis actually lies, we have indicated the nearest approximately parallel Cα-Cα bond using a backbone trace representation of the protein.

‡The deviation is the projection angle between the least-squares fit and the hinge axis found by Hingefind. The smaller this value is, the better the validity of the fit to that axis.

All of the expanded open states were also analyzed in terms of their pore radius profiles (using the program HOLE (Smart et al., 1997)). These profiles were similar for all five models. HOLE was also used to analyze the changes in volume of the central cavity region relative to the closed model. The expanded states show an increase of volume of the both the cavity and gate regions. The cavity is delimited by the mean *z*-coordinates of the threonine Cα atoms of the filter TVGYG motif (Thr65) to the mean *z*-coordinates of the more intracellular Thr107 ring. The gate region is defined as being from the Thr107 Cα *z*-coordinates to $z = -12$ Å, corresponding to the location of Val115. Using these definitions, the crystal (closed) structure has an interior cavity volume of 487 Å^3 and a gate region volume of 107 Å^3. The final structure from the equilibrated closed state has an interior cavity volume of 344 Å^3 and a gate region volume of 119 Å^3. For comparison, the expanded states have a mean cavity volume of 429 ± 50 Å^3 and a mean gate region volume of 719 ± 127 Å^3. Thus the cavity volume does not change significantly upon expansion of the channel, but the gate region volume increases by approximately sevenfold. Thus, the gate region volume in the expanded state is more than enough to accommodate a K^+ ion plus a first solvation shell (which has a volume of ~330 Å^3).

Characterization of the relaxed open-state model

As the initial models are produced by a steered process, we wanted to explore to what extent the conformation of the protein would return to its closed state after removal of the perturbing sphere. To do this we took the Ex3, Ex4, and Ex7 expanded models, removed the sphere, and ran an additional (unsteered) simulation for 5 ns. Ex4 and Ex7 represent the limits of successful expansion positions. An interesting comparison can be made at this stage if one just uses the Cα carbon atoms in the program HOLE to generate a pseudo pore radius profile corresponding to just the Cα traces of the models. Such a calculation confirms that the main chain of the protein moves in addition to the side chains. Fig. 4 *A* compares the profile from the crystal structure with the profiles from the expanded states, revealing a number of features. First, the radius profiles are very similar in the filter region and the upper region of the cavity. It is only in the lower (intracellular) section of the cavity (at $z \approx 14$ Å)

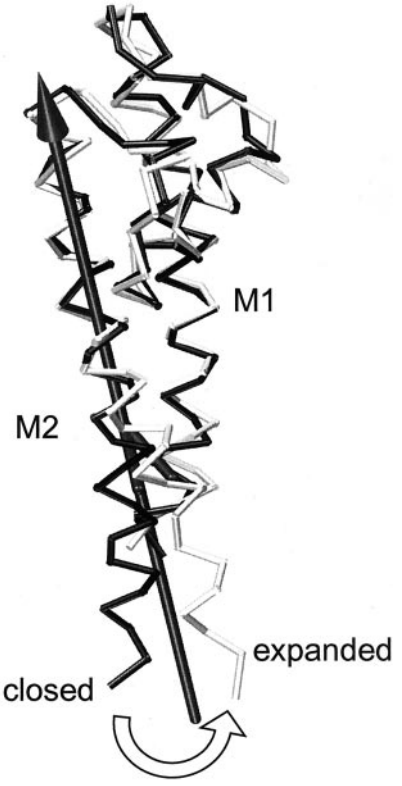

FIGURE 3 Hingefind results for expansion simulation Ex3. Chain B (from simulation Ex3; see Table 1) viewed toward the selectivity filter along an approximate normal to the pore (z) axis. The movement of the M2 helix about the effective hinge axis as determined by Hingefind is indicated by the arrow. This corresponds to the channel changing from a closed (*black*) to an expanded (*white*) state.

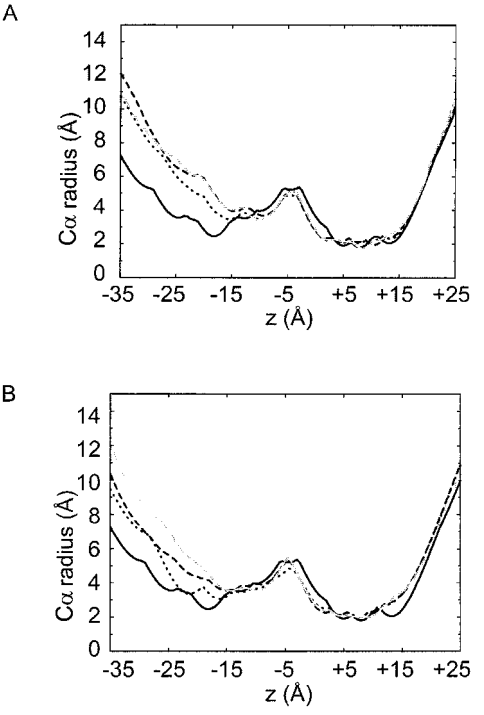

FIGURE 4 Pore radius profiles derived from Cα carbons only. (*A*) Comparison of the profile formed from the crystal structure (*solid black line*) with the expanded simulations Ex7 (sphere at −15.5 Å; *solid gray line*), Ex4 (sphere at −9.5 Å; *black dotted line*), and Ex3 (sphere at −14 Å; *black dashed lines*). (*B*) With the same lines as in *A*, but after an additional 5 ns of unsteered molecular dynamics.

and below that the Cα carbons move. This section is situated intracellularly to the Gly104 in the M2 helix. Second, it is notable that the different sphere positions result in similar expansion profiles. Upon removal of the sphere (Fig. 4 *B*), there is some relaxation of the Cα positions, but they do not return to positions that resemble the closed state (i.e., crystal structure).

For brevity, the following discussion refers to the Rx1 simulation, which was extended to 11 ns in total. Examination of the Cα RMSD of the protein relative to the expanded conformation (Fig. 5) suggests that the protein has relaxed to a stable state at ~2.5 ns, after which time there is little additional drift in the structure. A breakdown of the Cα RMSD into the various helical components revealed that the most significant deviation was observed in the M2 helix of chain C and chain D. The component RMSDs had stabilized fully after 5 ns.

We thus used the last 6 ns of this simulation as the basis for further analysis. In the remainder of the paper we refer to this stable state as the relaxed structure. How does this state differ from the expanded state and also from the closed state? Visual comparison of the closed, expanded, and related (i.e., $t = 11$ ns) structures showed that the M2 helices occupied a location intermediate between the expanded and closed-state models shown in Fig. 2 *A*. We were most interested in the pore radius profiles of the three states (Fig. 6 *A*). There are some important features to note regarding these profiles. First, the radius profile of the filter region does not change appreciably between these three states,

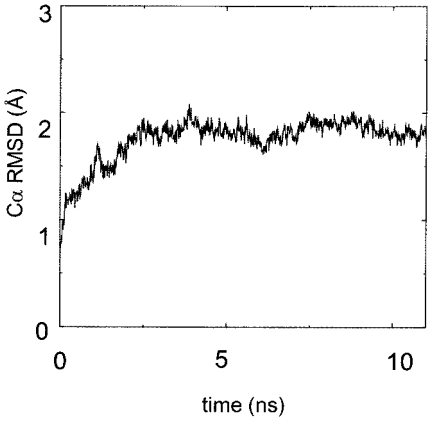

FIGURE 5 Structural drift during simulation Rx1. The RMSD of the Cα carbons relative to the expanded structure (Ex3 at $t = 1$ ns) is shown versus time.

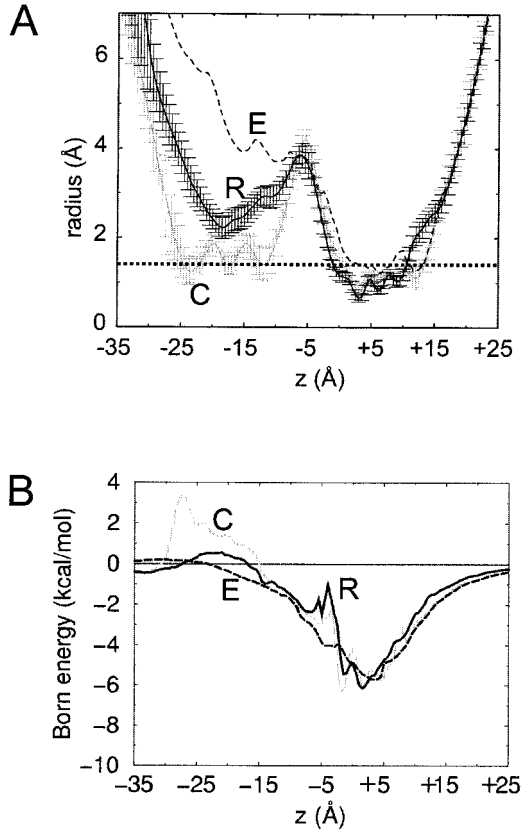

FIGURE 6 Comparison of the closed, expanded, and related state models of KcsA. (*A*) Pore radius profiles. The light gray line with error bars (*C*) represents the pore radius for a closed state of the channel, averaged (±SD) from a 1-ns simulation based upon the crystal structure. The dashed line (*E*) is the radius profile obtained from the final structure of simulation Ex3. The black line with error bars (*R*) represents the pore radius of for simulation Rx1, averaged (±SD) over the last 6 ns. The horizontal dotted line indicates the Pauling radius of a K^+ ion. (*B*) Born energies calculated relative to the bulk solvent value, indicated by the dotted straight line at zero kcal/mol. The dashed line (*E*) is the Born energy profile obtained from the final structure of simulation Ex3, the gray line (*C*) is the profile obtained from the closed state of the channel, and the solid line (*R*) is that obtained from the simulation Rx1 where structure has relaxed from the expansion phase. The dashed line (*E*) does tend toward zero but not as quickly as the M2 region of the expanded phase extends further into the cytoplasm. The apparent smoothing out in the filter region can be explained by the fact that toward the end of the expansion phase one of the amide groups had flipped around thus enabling a slightly larger pore radius in this region as can be seen in Fig. 6. The small differences at −35 Å are due to the proximity of the E118 groups, which are closer to the center of the channel and thus create a shallow favorable well. In the expanded state these groups are pushed further out, and due to the helix movement, the R117 groups have more influence on the energy here.

other than some small changes at the extracellular mouth of the pore. The latter are intriguing given that various authors (Chapman et al., 2001; Lu et al., 2001) have suggested that channel opening may be correlated with subtle changes in the conformation of the selectivity filter. However, as noted by Mackinnon (Morais-Cabral et al., 2001), such changes in the filter may require changes in the K^+ occupancy. The central cavity region has the same radius in all three states. The gate region in the relaxed structure is narrower than in the expanded state but with a minimum radius of ~2.3 Å is significantly wider than the closed state (minimum radius ~1 Å). Thus, the narrowest region of the gate in the relaxed-state model of KcsA is sufficiently wide to permit exit/entry of a solvated K^+ ion. This is shown by analysis of pore volumes for the relaxed state, which has a cavity volume of 364 $Å^3$ and a gate region volume 339 $Å^3$, both greater than the ~330 $Å^3$ occupied by a solvated (first hydration shell) K^+ ion. The relaxed states typically have a total of ~50 water molecules that make a continuous column of water from the selectivity filter to the intracellular water bath.

Is this enough to account for gating of the channel? A first approximation to an answer to this question may be obtained via evaluation of the Born energy profile for moving a single K^+ ion along the pore axis. Although there are some theoretical problems in using this simple model of ionic solvation (Rashin and Honig, 1985; Roux et al., 2000), especially in the selectivity filter region, it provides a semi-quantitative measure of the energetics of a K^+ ion as it is moved through the gate region of KcsA in the three models. We have compared Born energy profiles for the three models (Fig. 6 *B*) and for the x-ray structure (data not shown). For all four structures the Born energy profiles show the same minimum close to the filter and the focus of the P-helices (Roux and MacKinnon, 1999). The profile within the filter region is less physically meaningful as potassium channels are known to conduct with more than one ion within the pore at any one time (Morais-Cabral et al., 2001, Bernèche and Roux, 2001), but the profiles do provide an indication of the effects of the movements. The major differences are in the region of the intracellular gate (Figs. 7 and 8). For the x-ray structure and closed-channel model there is a barrier of ~6–8 kT in this region, sufficient to prevent ion permeation. In the expanded model there is no barrier at all, and in the relaxed model the barrier is ~1 kT. Thus, a relatively small difference in conformation between the closed and expanded state seems to be sufficient to account for gating of the channel.

Comparison with experimental data

It is important to compare our model(s) of the KcsA open state with available experimental data. The latter fall into two classes: data on block of KcsA channels by intracellular tetraalkylammonium ions and structural data derived from site-directed spin labeling experiments.

Data on KcsA channel block by tetraalkylammonium ions applied from the intracellular side indicate that tetrapentylammonium ions can block the channel in the open state (Heginbotham, 2001). Are our models of the open state of the KcsA channel able to accommodate such a molecule? If one considers properties such as the minimum effective

TABLE 3 Geometric properties for tetra-alkylammonium ions

Molecule	R_{GYR} (Å)	$g(r)$ peak (Å)	VDW radii (Å)
TEA	1.7 (0.1)	2.6	4.2 (0.03)
TPrA	2.4 (0.1)	3.9	5.4 (0.07)
TBA	2.9 (0.1)	5.1	6.4 (0.08)
TPeA	3.3 (0.2)	6.4	7.6 (0.27)

Values were calculated from 1-ns simulation in a 40-Å^3 box of SPC water. VDW, van der Waals; TEA, tetraethylammonium; TPrA, tetrapropylammonium; TBA, tetrabutylammonium; TPeA, tetrapentylammonium. Values quoted are mean values over the 1-ns simulation. Numbers in brackets reflect the SDs. The $g(r)$ values are calculated as the distribution of the terminal carbon atoms from the central nitrogen. The van der Waals distances are the radii of the smallest sphere that would encompass the solute. It should be remembered that the tetra-alkylammonium ions are not spherical (rather, they are ellipsoid) and are easily deformable.

radius (i.e., the smallest radius of sphere that would encompass the solute), $g(r)$, and the radius of gyration of a tetraalkylammonium ion, then a simple comparison can be made by performing simulations of these ions in bulk solution. Table 3 summarizes these data. These radii should be compared with minimum radii in the intracellular gate region of <1.3, ~ 2.3, and ~ 3.7 Å for the closed, relaxed, and expanded (Ex3) models, respectively. Thus, it appears that the expanded model could allow up to tetrapropylammonium (TPrA) to pass through the gate into the cavity that is the presumed site of block (Zhou et al., 2001), whereas for the relaxed model one might assume the cutoff to be at tetraethylammonium (TEA). However, it must be remembered that these tetraalkyl molecules are quite deformable and are capable of nonspherical, ellipsoid conformations. It is conceivable that some further distortion of the channel, along with side-chain fluctuations as well as some deformation of the blockers, may be needed for the larger tetraalkylammonium (TAA)s to access the cavity, and indeed initial steered MD simulations results indicate this is a possibility (unpublished). It may be possible to test this hypothesis via detailed comparison of the strength of voltage dependence of block of KcsA by the different TAAs.

A structural model for an open state has been derived from analysis of EPR spectra from KcsA subjected to site-directed spin labeling (Perozo et al., 1998, 1999). We have compared our relaxed-model structure with this model(Fig. 9). Two qualitative features emerge: 1) our model is less symmetric than that of Perozo, with only three of the four M2 helices deviating significantly from their conformation in the closed state, and 2) for those three M2 helices in the relaxed model that move away from their positions in the closed state, they move in the same direction in our simulations. Thus, the simulation-derived model is in broad agreement with that derived from EPR data. In both models the M2 helices show small distortions in the vicinity of Gly104 and move apart in the same manner. The differences between the simulation- and EPR-derived models may reflect, inter alia, spin-label-induced distortions and limitations of the simulations (see below). In addition to the comparison with the KcsA experimental data, Johnson and Zagotta (2001) have demonstrated how a similar rotational motion is observed in the cyclic nucleotide-gated channels.

Selectivity filter

Throughout the 11-ns relaxed structure simulation the behavior of the selectivity filter and the ions within it appears to be indistinguishable from that in previous simulations based on the closed state. The positions of the potassium ions in the filter remained more or less fixed relative to the carbonyl oxygens of the TVGYG motif. The third potassium ion remained in the cavity.

This result is relevant in the context of the many simulation studies (Aqvist and Luzhkov, 2000; Allen et al., 2000; Bernèche and Roux, 2000; Guidoni et al., 1999; Shrivastava and Sansom, 2000) that have addressed issues

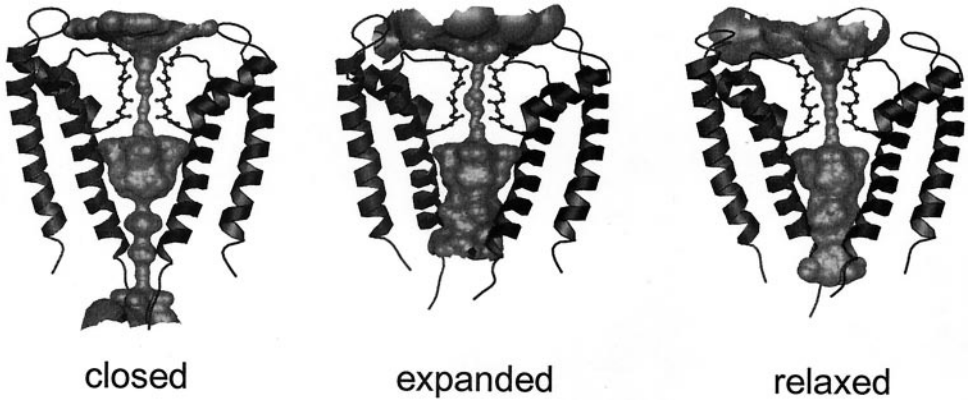

FIGURE 7 The inner surface of the pore for the three model states: closed (the final structure after 1 ns of simulation based upon the crystal structure), expanded (the final structure after simulation Ex3), and relaxed (Rx1 after 11 ns of simulation). Inner surfaces were generated with HOLE (Smart et al., 1997) and rendered within Molscript (Kraulis, 1991) and POV-Ray.

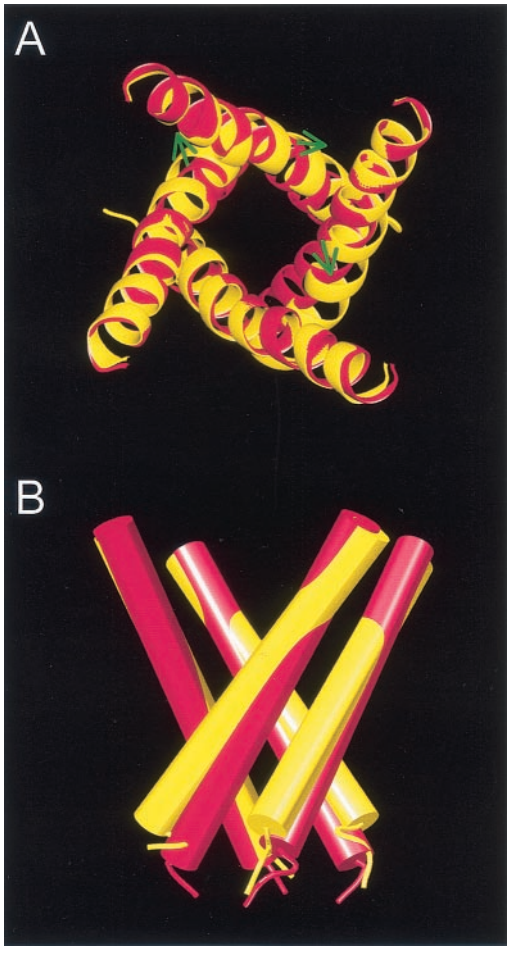

FIGURE 8 Superimposition of the M2 helices from the closed (*red*) and relaxed (*yellow*) models. The M2 helices were superimposed on residues before the G104 of the putative hinge (see above). (*A*) View looking down the pore axis from the filter toward the intracellular mouth of the channel. The green arrows provide a qualitative indication of the direction of motion of the helices. (*B*) View down a perpendicular to the pore axis, with the extracellular (filter) end of the helices at the top and the intracellular (gate) end of the helices at the bottom.

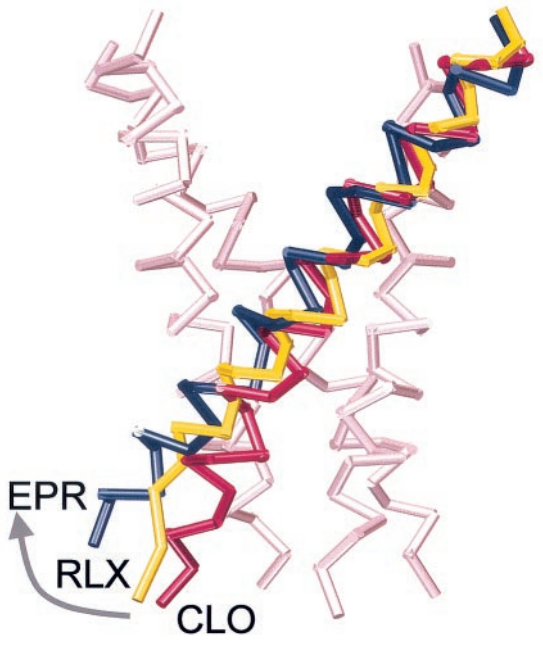

FIGURE 9 Comparison of the closed (*CLO*; *red*) and relaxed (*RLX*; *yellow*) models from this simulation study with a model of the open state (*EPR*; *blue*) derived from site-directed spin-labeling experiments (Liu et al., 2001) (RCSB codes 1JQ1 and 1JG2). Coordinates were kindly provided by E. Perozo. Only the M2 helices are shown, with their N-termini at the top. One M2 helix from each of the three models is compared; the other three M2 helices of the closed model are shown for reference (*pale pink*).

of KcsA permeation and selectivity based on the closed-state structure. Underlying such simulations is the assumption that the conformational behavior of the filter region is not significantly altered by the opening of the cytoplasmic gate. Our data seem to support this.

DISCUSSION

Selectivity filter

In this study we have used steered MD simulations in an attempt to develop a model of an open state of the KcsA channel. What are the arguments for and against such an approach? The main advantage of using steered MD to model an open state is that the model is generated in the presence of all of the interactions between main-chain and side-chain atoms within the (truncated) KcsA structure. Thus, the use of the expanding-sphere approach enables us to combine movement of the M2 helices (as indicated by the experimental data) with interactions of these helices with the rest of the protein during the opening process. Furthermore, the extended (11-ns) relaxation simulation enabled the expanded model to relieve any conformational distortions that may have occurred during the relative short expansion simulation.

Our main reservations concerning this model are as follows. First, the expansion phase is quite short, leading to questions regarding sampling of possible open states. We have tried to address this both by running multiple expansion simulations and by the relaxation simulation mentioned above. However, it remains an issue that will merit further exploration. Perhaps a more serious reservation is the use of a truncated structure for KcsA, based on the x-ray structure from which the first 22 and last 41 residues are missing. It has been shown by Cortes et al. (2001) that to some degree C-terminal truncation of KcsA does not lead to loss of gating. However, it would be of interest to develop an all-atom model of the complete KcsA tetramer (C. Capener and M. S. P. Sansom, unpublished results) based on the EPR-derived Cα model (Research Collaboratory for Struc-

tural Bioinformatics references 1JQ1 and 1JG2) and to use this in additional steered MD simulations.

Biological relevance

The biological relevance of this work is that it provides us with a plausible all-atom model of the open state of KcsA that appears to be consistent with experimental data, both from TAA block (Zhou et al., 2001) and spin-labeling (Perozo et al., 1998, 1999) data. This should enable us to explore, e.g., mechanisms of gating and block in more detail. In particular, we wish to explore the extent to which TAA blockers and/or the channel may have to undergo transient distortion for the blockers to access the internal cavity where they are thought to bind. This is related to the question of, e.g., how the inactivation particle accesses the cavity of Kv channels (Zhou et al., 2001). Of course, the structure of Kv channels in the gate region is likely to be rather different from that of KcsA (Camino et al., 2000; Sansom and Weinstein, 2000), but it may also be possible to explore Kv and other potassium channels via steered MD simulations.

Our model should also enable us to explore the process of gating per se of KcsA in a little more detail. In particular, we may be able to explore whether multiple metastable open states of the channel are possible. This is important given the debate as to whether (Meuser et al., 1999) or not (LeMasurier et al., 2001) KcsA exhibits sub-conductance levels. In this respect it may be useful to combine modeling of the open state(s) with Brownian dynamics (Allen and Chung, 2001) simulations of permeation and comparison with physiological data.

Note added in proof

During the submission of this manuscript, the structure of a related bacterial potassium channel gated by calcium ions, MthK was solved with x-ray crystallography by MacKinnon and colleagues (Jiang et al., 2002a). The x-ray structure reveals that the inner, M2, helices do indeed swing out. In fact, they have swung out substantially compared with KcsA (Jiang et al., 2002b). The position of the inner helices in the MthK structure resembles our expanded states rather more closely than the relaxed states. Several features of our simulations are in agreement with the model for gating proposed on the two crystal structures. Although the magnitude of these movements in our simulations is less than that for the crystal structures, the overall direction and nature of the movement are in excellent agreement. Our suggestion that the hinge region is located between Gly99 and Gly104 seems also to be in agreement with the open-state crystal structure where the Gly99 is proposed to be the origin of the hinge. To help illustrate this, we have added in the form of supplementary information a movie similar in view to that presented by MacKinnon and colleagues (Jiang et al., 2002b) at our website (http://sansom.biop.ox.ac.uk/phil/kcsa_opening.html).

We gratefully acknowledge the Wellcome Trust for the funding of this work and the Oxford Supercomputing Center for computer facilities. Thanks to all our colleagues for their comments on this work. Thanks also to Lise Heginbotham and to Eduardo Perozo for discussions concerning KcsA.

REFERENCES

Allen, T. W., A. Bliznyuk, A. P. Rendell, S. Kuyucak, and S. H. Chung. 2000. The potassium channel: structure, selectivity and diffusion. *J. Chem. Phys.* 112:8191–8204.

Allen, T. W., and S. H. Chung. 2001. Brownian dynamics study of an open-state KcsA potassium channel. *Biochem. Biophys. Acta.* 1515: 83–91.

Aqvist, J., and V. Luzhkov. 2000. Ion permeation mechanism of the potassium channel. *Nature.* 404:881–884.

Armstrong, C. M. 1971. Interaction of tetraethyl-ammonium ion derivatives with the potassium channels of giant axons. *J. Gen. Physiol.* 58:413–437.

Armstrong, C. M. 1997. A closer picture of the K channel gate from ion trapping experiments. *J. Gen. Physiol.* 109:523–524.

Armstrong, C. M., and L. Binstock. 1965. Anomalous rectification in the squid giant axon injected with tetraethylammonium chloride. *J. Gen. Physiol.* 48:859–872.

Ashcroft, F. M. 2000. Ion Channels and Disease. Academic Press, San Diego.

Berendsen, H. J. C., J. P. M. Postma, W. F. van Gunsteren, A. DiNola, and J. R. Haak. 1984. Molecular dynamics with coupling to an external bath. *J. Chem. Phys.* 81:3684–3690.

Berendsen, H. J. C., D. van der Spoel, and R. van Drunen. 1995. GROMACS: a message-passing parallel molecular dynamics implementation. *Comput. Phys. Commun.* 95:43–56.

Bernèche, S., and B. Roux. 2000. Molecular dynamics of the KcsA K^+ channel in a bilayer membrane. *Biophys. J.* 78:2900–2917.

Bernèche, S., and B. Roux. 2001. Energetics of ion conduction through the K^+ channel. *Nature.* 414:23–24.

Biggin, P. C., G. R. Smith, I. H. Shrivastava, S. Choe, and M. S. P. Sansom. 2001. Potassium and sodium ions in a potassium channel studied by molecular dynamics. *Biochim. Biophys. Acta.* 1510:1–9.

Camino, D. D., M. Holmgren, Y. Liu, and G. Yellen. 2000. Blocker protection in the pore of a voltage-gated K^+ channel and its structural implications. *Nature.* 403:321–325.

Chapman, M. L., H. S. Krovetz, and A. M. J. VanDongen. 2001. GYGD pore motifs in neighbouring potassium channel subunits interact to determine ion selectivity. *J. Physiol.* 530:21–33.

Cortes, D. M., L. G. Cuello, and E. Perozo. 2001. Molecular architecture of full-length KcsA: role of cytoplasmic domains in ion permeation and activation gating. *J. Gen. Physiol.* 117:165–180.

Davis, M. E., J. D. Madura, B. A. Luty, and J. A. McCammon. 1991. Electrostatics and diffusion of molecules in solution: simulations with the University of Houston Brownian dynamics program. *Comput. Phys. Commun.* 62:187–197.

Doyle, D. A., J. M. Cabral, R. A. Pfuetzner, A. Kuo, J. M. Gulbis, S. L. Cohen, B. T. Cahit, and R. MacKinnon. 1998. The structure of the potassium channel: molecular basis of K^+ conduction and selectivity. *Science.* 280:69–77.

Flynn, G. E., and W. N. Zagotta. 2001. Conformational changes in S6 coupled to the opening of cyclic nucleotide-gated channels. *Neuron.* 30:689–698.

Forrest, L. R., and M. S. P. Sansom. 2000. Membrane simulations: bigger and better? *Curr. Opin. Struct. Biol.* 10:174–181.

Grubmuller, H., B. Heymann, and P. Tavan. 1996. Ligand binding: molecular mechanics calculation of the streptavidin-biotin rupture force. *Science.* 271:997–999.

Guidoni, L., V. Torre, and P. Carloni. 1999. Potassium and sodium binding to the outer mouth of the K^+ channel. *Biochemistry.* 38:8599–8604.

Hayward, S., and H. J. C. Berendsen. 1998. Systematic analysis of domain motions in proteins from conformational change: new results on citrate synthase and T4 lysozyme. *Protein Struct. Funct. Genet.* 30:144–154.

Hayward, S., A. Kitao, and H. J. C. Berendsen. 1997. Model-free methods of analyzing domain motions in proteins from simulation: a comparison of normal mode analysis and molecular dynamics simulation of lysozyme. *Protein Struct. Funct. Genet.* 27:425–437.

Heginbotham, L. 2001. Blockade of the KcsA K^+ channel by quaternary ammonium compounds. *Biophys. J.* 80:212a.

Heginbotham, L., M. LeMasurier, L. Kolmakova-Partensky, and C. Miller. 1999. Single *Streptomyces lividans* K^+ channel: functional asymmetries and sidedness of proton activation. *J. Gen. Physiol.* 114:551–559.

Hermans, J., H. J. C. Berendsen, W. F. van Gunsteren, and J. P. M. Postma. 1984. A consistent empirical potential for water-protein interactions. *Biopolymers.* 23:1513–1518.

Hess, B., J. Bekker, H. J. C. Berendsen, and J. G. E. M. Fraaije. 1997. LINCS: a linear constraint solver for molecular simulations. *J. Comp. Chem.* 18:1463–1472.

Hille, B. 1992. Ionic Channels of Excitable Membranes, 2nd ed. Sinauer Associates, Sunderland, MA.

Humphrey, W., A. Dalke, and K. Schulten. 1996. VMD: visual molecular dynamics. *J. Mol. Graph.* 14:33–38.

Israelewitz, B., M. Gao, and K. Schulten. 2001. Steered molecular dynamics and mechanical functions of proteins. *Curr. Opin. Struct. Biol.* 11: 224–230.

Jiang, Y., A. Lee, J. Chen, M. Cadene, B. Chait, and R. MacKinnon. 2002a. Crystal structure and mechanism of a calcium-gated potassium channel. *Nature.* 417:515–522.

Jiang, Y., A. Lee, J. Chen, M. Chadene, B. Chait, and R. MacKinnon. 2002b. The open pore conformation of potassium channels. *Nature.* 417:523–526.

Johnson, J. P., and W. N. Zagotta. 2001. Rotational movement during cyclic nucleotide-gated channel opening. *Nature.* 412:917–921.

Kabsch, W., and C. Sander. 1983. Dictionary of protein secondary structure: pattern recognition of hydrogen-bonded and geometrical features. *Biopolymers.* 22:2577–2637.

Kraulis, P. J. 1991. MOLSCRIPT: a program to produce both detailed and schematic plots of protein structures. *J. Appl. Cryst.* 24:946–950.

LeMasurier, M., L. Heginbotham, and C. Miller. 2001. KcsA: it's a potassium channel. *J. Gen. Physiol.* 118:303–313.

Liu, Y.-S., P. Sompornpisut, and E. Perozo. 2001. Structure of KcsA intracellular gate in the open state. *Nat. Struct. Biol.* 8:883–887.

Lu, T., A. Y. Ting, J. Mainland, L. Y. Jan, P. G. Schultz, and J. Yang. 2001. Probing ion permeation and gating in a K^+ channel with backbone mutations in the selectivity filter. *Nat. Neurosci.* 4:239–246.

MacKinnon, R., S. L. Cohen, A. Kuo, A. Lee, and B. T. Chait. 1998. Structural conservation in prokaryotic and eukaryotic potassium channels. *Science.* 280:106–109.

Meuser, D., H. Splitt, R. Wagner, and H. Schrempf. 1999. Exploring the open pore of the potassium channel from *Streptomyces lividans. FEBS Lett.* 462:447–452.

Morais-Cabral, J. H., Y. Zhou, and R. MacKinnon. 2001. Energetic optimization of ion conduction rate by the K^+ selectivity filter. *Nature.* 414:37–42.

Perozo, E., D. M. Cortes, and L. G. Cuello. 1998. Three-dimensional architecture and gating mechanism of a K^+ channel studied by EPR spectroscopy. *Nat. Struct. Biol.* 5:459–469.

Perozo, E., D. M. Cortes, and L. G. Cuello. 1999. Structural rearrangements underlying K^+ channel activation gating. *Science.* 285:73–78.

Procacci, P., T. Darden, and M. Marchi. 1996. A very fast molecular dynamics method to simulate biomolecular systems with realistic electrostatic interactions. *J. Phys. Chem.* 100:10464–10468.

Rashin, A., and B. Honig. 1985. Reevaluation of the Born model of ion hydration. *J. Phys. Chem.* 89:5588–5593.

Roux, B., S. Berneche, and W. Im. 2000. Ion channels, permeation and electrostatics: insight into the function of KcsA. *Biochemistry.* 39: 13295–13306.

Roux, B., and R. MacKinnon. 1999. The cavity and pore helices in the KcsA K^+ channel: electrostatic stabilization of monovalent cations. *Science.* 285:100–102.

Sansom, M. S. P., and H. Weinstein. 2000. Hinges, swivels and switches: the role of prolines in signalling via transmembrane alpha helices. *Trends Pharmacol. Sci.* 21:445–451.

Shrivastava, I. H., C. Capener, L. R. Forrest, and M. S. P. Sansom. 2000. Structure and dynamics of K^+ channel pore-lining helices: a comparative simulation study. *Biophys. J.* 78:79–92.

Shrivastava, I. H., and M. S. P. Sansom. 2000. Simulations of ion permeation through a K channel: molecular dynamics of KcsA in a phospholipid bilayer. *Biophys. J.* 78:557–570.

Shrivastava, I. H., and M. S. P. Sansom. 2002. Molecular dynamics simulations and KcsA channel gating. *Eur. Biophys. J.* 31:207–216.

Smart, O. S., J. Breed, G. R. Smith, and M. S. P. Sansom. 1997. A novel method for structure-based prediction of ion channel conductance properties. *Biophys. J.* 72:1109–1126.

Smart, O. S., J. M. Goodfellow, and B. A. Wallace. 1993. The pore dimensions of gramicidin A. *Biophys. J.* 65:2455–2460.

Smart, O. S., J. G. Neduvelil, X. Wang, B. A. Wallace, and M. S. P. Sansom. 1996. Hole: a program for the analysis of the pore dimensions of ion channel structural models. *J. Mol. Graph.* 14:354–360.

Wriggers, W., and K. Schulten. 1997. Protein domain movements: Detection of rigid domains and visualization of hinges in comparison of atomic coordinates. *Protein Struct. Funct. Genet.* 29:1–14.

Zhou, M., J. H. Morais-Cabral, S. Mann, and R. MacKinnon. 2001. Potassium channel receptor site for the inactivation gate and quaternary amine inhibitors. *Nature.* 411:657–661.